Numerical Study on Development of Hysteretic Model for Stiffened Steel Shear Panel Dampers

Zhiyi Chen*, Hanbin Ge**, Tsutomu Usami ***

* Graduate Student, Dept. of Civil Eng., Nagoya University, Furo-cho, Chikusa-ku, Nagoya 464-8603
** Dr. of Eng., Associate Professor, Dept. of Civil Eng., Nagoya University, Furo-cho, Chikusa-ku, Nagoya 464-8603
***Dr. of Sc., Dr. of Eng., Professor, Dept. of Civil Eng., Nagoya University, Furo-cho, Chikusa-ku, Nagoya 464-8603

The paper presents a hysteretic model for stiffened steel shear panel dampers (SPD). To explore shear behavior of such dampers, nonlinear analyses have been conducted on elaborate finite element models subjected to cyclic shear loading, in which a modified two-surface model is incorporated to trace the material nonlinearity. Initial geometric imperfections and residual stresses are also taken into account. An extensive parametric study is performed to investigate the influences of design parameters on the ultimate shear strength and ductility capacity. Based on numerical results, empirical formulae accounting for the contributions of both web and flanges are proposed and checked with available experimental data. Finally, a simplified bilinear hysteretic model for SPD is presented for further use in the time-history analysis of engineering structures installed with such dampers.

Key Words: stiffened steel shear panel damper, strength, ductility, hysteretic model

1. Introduction

Shear-type hysteretic damper (stiffened or unstiffened) is one type of metallic yield damper, whose effective mechanism for dissipation of energy input to a structure from an earthquake is through inelastic deformation of the metals[1]. The conventional forms of shear-type hysteretic damper incorporated into building structures are shown in Fig.1. For shear-wall type damper, see Fig.1 (c), the web plate is much slender. Consequently, web local buckling occurs prior to yielding. Post-buckling strength may be fully utilized due to the tension-field action developed subsequently in diagonal region. For the other two types as shown in Fig.1 (a) and (b), local buckling should be avoided because it is one of the main factors that cause deterioration of energy dissipation capacity. This is not preferable for shear panels acting as energy dissipator against major earthquakes. In other words, the web thickness of the shear panels in such structural systems should be designed much stockier than that of shear-wall type dampers as possible to make web yielding prior to buckling. Although extensive experimental and analytical researches have been conducted on shear-type hysteretic dampers and building structures installed with such dampers[2)-6)], the researches on bridge structures remain infancy[7),8)]. Considering requirements of transportation space and aesthetic demands for bridge structures, only types (a) and (b) are concerned in the present study. These dampers are referred to as shear panel or shear panel damper later.

One consideration in this paper is the material of shear panel. Previously published researches about shear panels focused on those made of low-yield steel[2)-4)]. However, at present this kind of low-yield steel has not yet been included in standard codes, such as JIS (Japanese Industrial Standards)[9)] and ASTM (American Society of Testing and Materials)[10)]. Because of the immaturity of low-yield steel in the material market and limited guide for low-yield steel in specifications, the conventional mild steel JIS SS400 (equivalent to ASTM A36) is considered in this study.

In addition to the steel material, the shear panel dampers considered here are stiffened with longitudinal and transverse stiffeners. As mentioned above, the web of steel shear panel dampers must yield prior to buckling. Thus, relatively small width-thickness ratio is generally required. Stiffeners can serve for this purpose without change the dimension size of one shear panel damper. Meanwhile, the decrease of web plate thickness improves the ductility of the shear panel damper. In other words, the yield strength of shear panel dampers is related to the cross section area of one panel while ductility capacity is related to the web slenderness of subpanel divided by stiffeners. However all these merits are verified by earlier experimental studies on

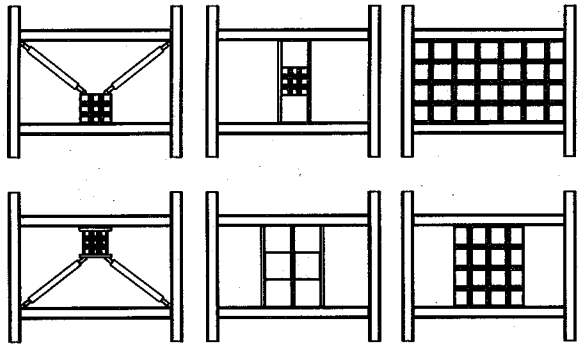

Fig.1 Samples of shear-type hysteretic dampers incorporated into framed structures: (a) combined-type; (b) inner column-type; and (c) shear wall-type

stiffened shear panels made of low-yield steel[2),3)] or unstiffened shear panels made of conventional steel[5),6)]. In addition, there are still no clear specifications on design of stiffener rigidity for shear panel dampers. In view of this, parametric study has been carried out. A suitable parameter range for stiffener rigidity has been proposed based on the concept of optimum rigidity of stiffener[11)] for practical design purposes.

So far, most of analyses concerning the shear panel dampers are limited within the scope of laboratory experiments, that is, a study deals with the phenomenological hysteretic behavior of shear panel dampers on the observation of behavior at member level. The main objective of this study is to make full use of numerical analysis to clarify the ultimate shear strength, ductility and hysteretic behavior of stiffened steel shear panel dampers made of conventional steel, which are subjected to cyclic shear loading. Elaborate finite element models are established, in which a modified two-surface model developed in Nagoya University by Shen et al.[12),13)] is employed to trace the material nonlinearity. Initial geometric imperfections and residual stresses are also taken into account. To ensure stable seismic performance, an extensive parametric study is carried out to find a suitable range of design parameters for the shear panel dampers through large deformation analysis. Ultimate strength and ductility, especially the influence of flanges, are explored. Empirical formulae for stiffened shear panels are presented based on the numerical results and checked with available experimental data. Finally, a suitable bilinear hysteretic model for time-history analysis of stiffened shear panels is established based on the numerical results. The model is provided with two important characteristics: (1) it can simulate the hysteretic and energy dissipating behavior of the shear panel used as energy dissipators accurately without pinch and strength degradation; and (2) it is sufficiently simple that in turn it can be readily implemented in the time-history analysis of complicated structural systems in practical design.

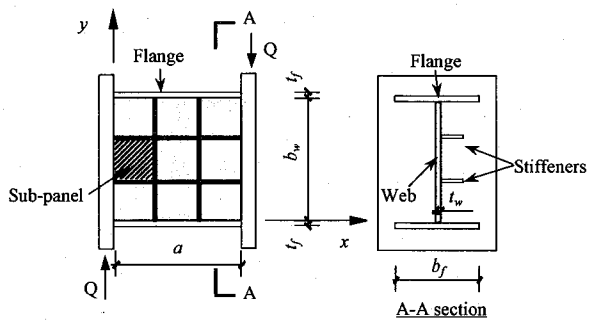

Fig.2 Stiffened shear panel with $n_L = n_T = 2$

2. Analytical Model

Fig.2 shows a typical shear panel damper, consisting of a stiffened steel plate, referred to as the web, and surrounding longitudinal and transverse boundary elements. The web is stiffened with two pairs of equidistant longitudinal and transverse stiffeners.

The shear panel damper is characterized by the web slenderness parameter, R_w, being defined as[14)]

$$R_w = \frac{b_w}{t_w}\sqrt{\frac{12(1-\nu^2)\tau_y}{k_s \pi^2 E}} \tag{1}$$

where b_w and t_w are the depth and thickness of the web, respectively, τ_y is shear yield stress of web material, $\tau_y = \sigma_y/\sqrt{3}$. E is the Young's modulus of elasticity, ν is the Poisson's ratio, and k_s is the elastic buckling coefficient of a simply-supported plate under shear, given by

$$k_s = \begin{cases} (n_L+1)^2(5.35+4/\alpha_s^2), & \alpha_s \geq 1 \\ (n_L+1)^2(5.35/\alpha_s^2+4), & \alpha_s < 1 \end{cases} \tag{2}$$

where n_L is the number of longitudinal stiffeners, α_s is the aspect ratio of a subpanel. Since the web considered is an equi-stiffened square plate, α_s is then equal to the aspect ratio of the web, α, defined as $\alpha = a/b_w$, where a is the web length.

Other important design parameters for SPD are: the flange to web thickness ratio, t_f / t_w, which represents the relative flange rigidity; the ratio of γ_s / γ_s^* represents the relative rigidity of stiffeners, where γ_s is rigidity of stiffener, given by Eq. (3) and γ_s^* stands for optimum rigidity of stiffener. γ_s^* is given by Eq. (4), defined at the point where the critical load of the stiffened plate is equal to the critical load of an individual simply-supported subpanel[11)].

$$\gamma_s = \frac{EI_s}{b_w D_w} \tag{3}$$

$$\gamma_s^* = \left(\frac{23.1}{(n_L+1)^{2.5}} - \frac{1.35}{(n_L+1)^{0.5}}\right)\frac{\left(1+\alpha^{3/(n_L+1)-0.3}\right)^{2(n_L+1)-1}}{1+\alpha^{5.3-0.6(n_L+1)-3/(n_L+1)}} \tag{4}$$

where I_s is the moment of inertia of the stiffener, taken at the interaction surface of stiffener and web, and D_w is flexural rigidities per unit width of the web.

The physical dimensions of analytical models are listed in

Table 1. Three series of stiffened shear panels with 1, 2, and 3 two-way stiffeners are investigated. R_w varies from 0.2 to 0.7. The web has the unit aspect ratio, α. The length, a, and the depth of the web, b_w, are equal to 1000mm. The flange width is fixed as 300mm, which is about 1/3 of the web depth. In this study, stiffeners are placed on one side to save cost for fabrication. The width-to-thickness ratio of stiffeners is taken as 9 to avoid local buckling. In BS5400[15], the value of 10 is specified for one-sided stiffeners, and in Guidelines for design of railway viaduct with dampers and braces in Japan[7], the value of 25 is specified for both-sided stiffeners.

The general-purpose finite element program, *ABAQUS*[16] is employed for large inelastic deformation analysis. A four-node doubly curbed, first order, reduced-integration shell element (S4R) is used. In numerical analysis, steel grade SS400 is used as the steel material. In order to trace the material cyclic behavior accurately, a two-surfaced model, developed in Nagoya University by Shen et al.[12),13)], is used. This material model was well testified by Gao et al.[17] and succeeded in estimate the cyclic shear behaviors of box and I-section girders[18),19)]. The present analytical method has been validated by comparing the numerical results with experimental results.

In this study, the distribution of the residual stresses in the web and the stiffeners is idealized in a rectangular pattern, based on experimental inspections and analytical study of plate assemblies[20], as shown in Fig.3. Preliminary analysis indicates that the residual stresses only influence the behavior of shear

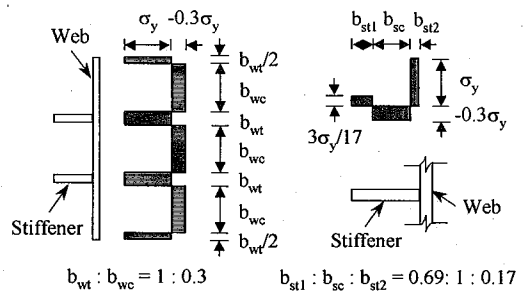

(a) Web (b) Stiffener

Fig.3 Distribution of residual stresses in the web and stiffeners

panels before yielding. For geometric imperfections, initial out-of-plane deflections distributed in a sinusoidal pattern is considered,

$$\delta_w = -\frac{a}{1000}\sin\left(\frac{\pi x}{a}\right)\sin\left(\frac{\pi y}{b_w}\right) + \frac{b_w}{150(n_L+1)}\sin\left(\frac{(n_L+1)\pi x}{a}\right)\sin\left(\frac{(n_L+1)\pi y}{b_w}\right) \quad (5)$$

The first and second terms in the equation represent the global and local initial deflections, respectively, whose amplitudes (a/1000, b_w/1500(n_L+1)) are obtained from the Japanese stability design guidelines[14].

Consider both ends of the panel are welded on considerably stiff plate in practice, the degrees of freedom of the model at the planes $x = 0$ and $x = a$ (see Fig.2) are assumed fixed except for

Table 1 Summary of stiffened shear panel dampers[a]

Dimensions							Analytical Results		Predictions	
n_L=n_T	R_w	b_w/t_w	t_w (mm)	t_f (mm)	b_f (mm)	t_s (mm)	τ_m/τ_y	$\sum E_i/E_e$	τ_u/τ_y	$\sum E_i/E_e$
	0.7	158	6.3	25.3	300	8.9	1.177	1110	1.163	-
	0.6	136	7.4	29.5	300	10.0	1.233	1209	1.208	-
n_L=n_T=1	0.5	113	8.84	35.4	300	11.4	1.297	1332	1.277	1465
	0.4	91	11.4	44.2	300	13.5	1.381	1473	1.397	1458
	0.3	68	14.7	44.2	533.3	16.7	1.511	1597	1.499	1453
	0.7	238	4.2	16.8	300	5.7	1.126	456	1.130	-
	0.6	204	4.9	19.6	300	6.4	1.202	1079	1.169	-
n_L=n_T=2	0.5	169	5.9	23.6	300	7.3	1.266	1297	1.231	1468
	0.4	137	7.3	29.2	300	8.7	1.348	1418	1.340	1462
	0.3	102	9.8	39.2	300	10.8	1.468	1561	1.422	1457
	0.2	67	15.0	60.0	300	14.6	1.585	1649	1.499	1453
	0.7	317	3.2	12.6	300	4.5	1.131	1023	1.114	-
	0.6	272	3.7	14.7	300	5.0	1.208	1241	1.150	-
n_L=n_T=3	0.5	226	4.4	17.7	300	5.8	1.278	1325	1.208	1470
	0.4	181	5.5	22.1	300	6.8	1.345	1444	1.311	1464
	0.3	136	7.4	29.5	300	8.4	1.465	1554	1.384	1459
	0.2	91	11.1	44.2	300	11.4	1.547	1612	1.442	1456

[a] Some of the parameters are kept constant as: $\alpha = 1.0$, $t_f/t_w = 4.0$, $\gamma_s/\gamma_s^* = 3.0$, $\sigma_y = 235\text{N/mm}^2$, and $b_s = 9t_s$, except for the case of $n_L = n_T = 1$ and $R_w = 0.3$, in which t_f is taken as $3t_w$ and b_f is taken as $(4/3)^2 \times 300$ mm.

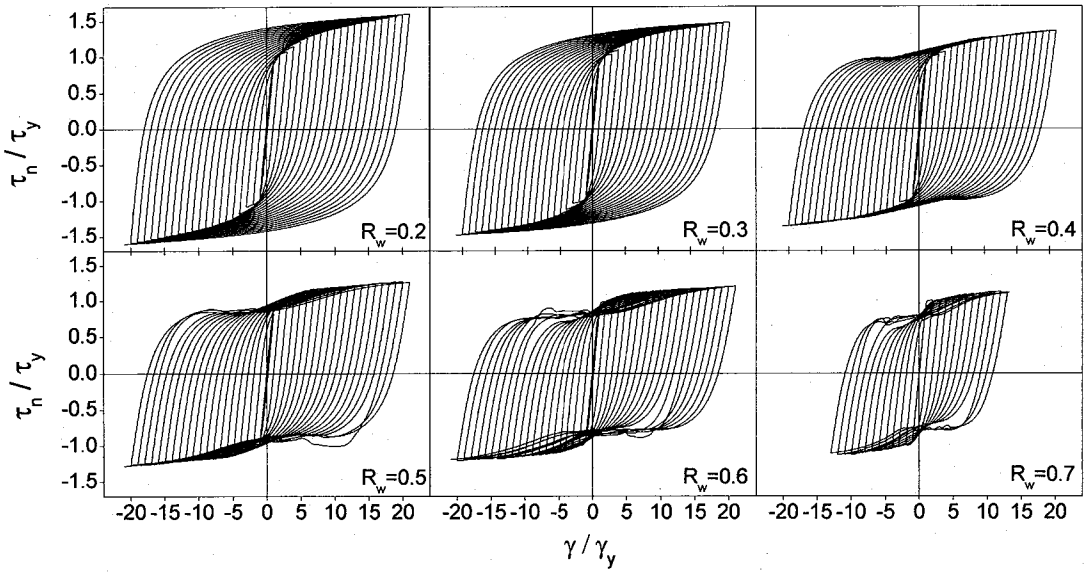

Fig.4 Hysteretic shear stress-shear strain curves ($n_L = n_T = 2$, $\gamma_s/\gamma_s^* = 3.0$, $\alpha = 1.0$, and $t_f/t_w = 4.0$)

the displacement in the x and y directions of the loading edge. Cyclic displacement loading pattern is considered here. The transverse displacement, Δ, is imposed along the plane $x = a$, as shown in Fig.2. The peak displacement in each cycle is the multiple of the yield displacement of the web in pure shear, Δ_y.

During the analysis, average shear stress, τ_n, and average shear strain, γ, are measured to evaluate shear strength and ductility of SPD as follows,

$$\tau_n = \frac{Q}{b_w t_w}, \quad \gamma = \frac{\Delta}{a} \tag{6}$$

where Q = summation of vertical reaction forces at the plane $x = 0$.

3. Hysteretic Performance and Ductility Capacity of Stiffened Shear Panel Dampers

To investigate the hysteretic behavior of SPD, a series of SPD with 1, 2 or 3 two-way stiffeners are conducted by cyclic analysis. The analytical results, such as maximum shear strength τ_m (normalized by τ_y) and cumulative dissipated energy ΣE_i (normalized by E_e) are summarized in Table 1. The definitions of ΣE_i and E_e are described later in section 6. It will be revealed in the parametric study later that when flange rigidity and web aspect ratio are satisfied with suggested ranges, i.e., $\gamma_s/\gamma_s^* \geq 3.0$, $t_f / t_w \geq 4.0$, and $0.5 \leq \alpha \leq 1.5$, the influences of these design parameters on load carrying capacity of the web can be ignored. Therefore the hysteretic performance and ductility capacity of stiffened shear panel dampers can be easily investigated into focus on the single design parameter, R_w, the web slenderness.

Fig.4 shows typical hysteretic curves of the normalized shear stress versus shear strain of SPD with $n_L = n_T = 2$ and R_w varying from 0.2 to 0.7. It is apparent that the hysteretic behavior of shear panels can be grouped into three types according to the value of R_w.

Generally speaking, the hysteretic loops of shear panels with stockier web (i.e., $R_w = 0.2$ and 0.3) are stable and the kinematical and isotropic effects are mixed together. A visible inelastic behavior occurs at a normalized shear stress of about 0.8. No plate buckling is observed. The whole steel web yields and achieves in full plastic manner gradually. Strain hardening begins at about $4\gamma_y$ and maintains up to the end of the analysis.

For shear panels with medium stockier web (i.e., $R_w = 0.4$ and 0.5), the hysteretic loops are stable too. Unlike the stockier web, the Bauchinger effect is significant. A visible inelastic behavior occurs at a normalized shear stress of about 0.8. Strain hardening begins at about $4\gamma_y$. At a displacement of $\gamma = +12\gamma_y$, a slight degree of pinch is observed in the case of $R_w = 0.5$ due to the occurrence of web buckling. However, tension field action prevents strength reduction. The out-of-plane displacement is measured as 15mm at the end of this loading circle. As seen from Fig.4, pinching phenomenon does not develop in the subsequent cycles and the average strength continues increasing till the termination of the analysis.

For those with slender webs (i.e., $R_w = 0.6$ and 0.7), relatively significant pinching phenomenon, which causes degradation of energy dissipating capacity, is observed. The pinch occurs as soon as $8–10\gamma_y$ is reached. Especially at the last few cycles, the curves become unsmooth, demonstrating the unstable behavior of shear panel in numerical analysis.

Seen from the view of ductility capacity, all the cases have good ductility up to 20 except for $R_w = 0.7$. In the case of $R_w = 0.7$, the shear strength began deteriorating at $\gamma / \gamma_y = 12$ after the peak of the ascending branch, and soon is terminated due to significant local buckling. The maximum residual out-of-plane deflection at the central panel zone is as large as 23.5 mm in this case, as is

over 5 times the web thickness.

When SPD is installed into structures acting as an energy dissipator, large deformation capacity, namely, excellent ductility capacity is usually required. For building structures, maximum story drift of 1/100 is usually specified for Level II design earthquake[15]. Thus, the range of 3/100–5/100 is taken as lower bound of ductility for a combined-type shear panel damper to be installed in such framed structures as shown in Fig.1 (a). The experimental researches[6] have shown that given $R_w \leq 0.55$, the ductility value of 5/100 could be met for shear panels made of low-yield steel (such as LYP100 and LYP235) under cyclic loading. However no available value is specified for bridge structures. Hence for shear panel dampers made of conventional steel such as SS400 to be installed into bridge structures, the lower bound of ductility is taken as $20\gamma_y$. It is considered that the steel material may fail in low-cycle fatigue beyond $20\gamma_y$ [21](about 3.4/100 for SS400). The numerical analyses are terminated manually at this limit value.

Consider stable hysteretic performance and ductility of SPD as well as feasibility in fabrication, $0.2 \leq R_w \leq 0.5$ is recommended for SPD in practical design.

4. Parametric Study

Parametric study is carried out to survey the design parameters' effects on the hysteretic behavior of shear panel dampers. The parameters considered in this section are the flange rigidity, t_f / t_w, the stiffener rigidity, γ_s / γ_s^*, and the web aspect ratio, α. Although the study is restricted on shear panels with two pairs of stiffeners and web slenderness parameter of $R_w = 0.4$, which is a typical value for shear panels, the obtained findings can also be applied to the R_w range from 0.2 to 0.5

4.1 Effects of flange rigidity, t_f / t_w

Effects of flange rigidity have long been investigated since the diagonal tension theory for plate girders with rigid flanges and very thin web. In practice design, it is generally accepted that heavier flanges could provide sufficiently rigid anchors to the web as to ensure the full development of tension field and remain postbuckling strength as well. Hence, location of plastic hinges in the flanges are considered into the ultimate shear strength to reflect the influence of bending stiffness of the flanges on the load carrying capacity of plate girders[22]. However, as web thickness increases, such as in the case of shear panel damper, the contribution of tension field to the strength capacity decreases, while the contribution of heavier flanges increases. This phenomenon has been testified by several experiments[6,8]. In this section, parametric study is carried out to attempt to reconsider the influence of flange rigidity. The relative flange rigidity is denoted by t_f / t_w which is the flange to web thickness ratio. The influence of flange rigidity on the shear carrying capacity of the web and that of total shear panel is examined by varying the flange thickness. Design parameters with $n_L = n_T = 2$, $R_w = 0.4$, and $\gamma_s / \gamma_s^* = 3.0$ are used. The thickness of flanges are varied as 58.4mm, 29.2mm, 14.6mm, and 7.3mm for $t_f / t_w = 8, 4, 2$, and 1, respectively.

The envelopes of obtained normalized shear strength versus shear strain cyclic curves are shown in Fig.5 (a). These envelopes are obtained by plotting the peak shear strain of each cycle along with the corresponding shear stress averaged from positive and negative loading sides. To better understand the contributions of the flanges and the web to the shear panel's ultimate strength, the curves in Fig.5 (a) are decomposed into two components, one being carried by the web and the other being carried by the flanges, as shown in Fig.5 (b) and (c), respectively. Seen from Fig.5 (b), the curve of $t_f / t_w = 1$ shows obvious drop after peak strength, indicating that web buckling occurred. That is, the flanges with $t_f / t_w = 1$ are not stiff enough to restrain rotations of web edges. In the other three cases, the shear forces carried by the webs are almost equal at the ultimate state. Especially for the stockier flanges ($t_f / t_w = 4$ and 8), the behaviors are almost analogous with each other during entire loading process. These results imply that $t_f / t_w = 2$ is stiff enough to provide higher degree of restraint at the flange-web juncture so as to ensure the

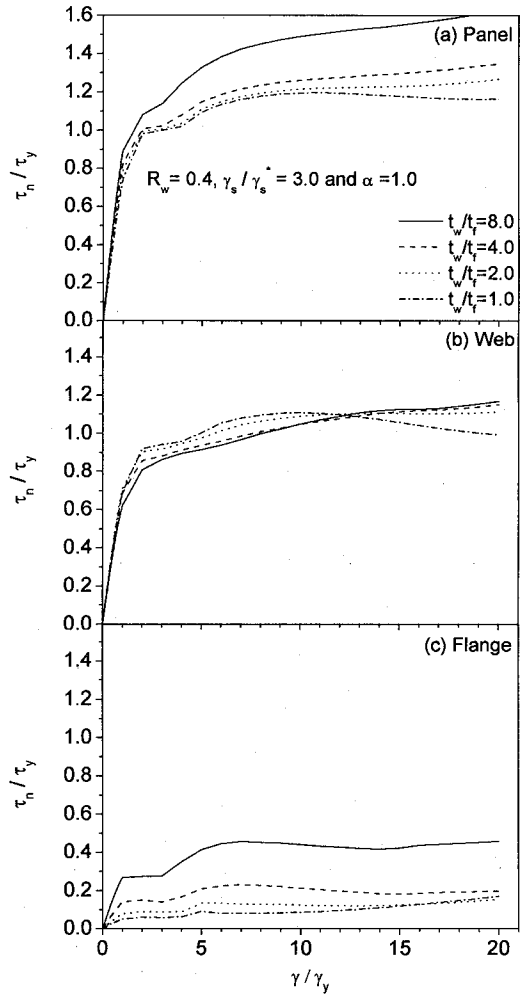

Fig.5 Effects of flange rigidity, t_f / t_w

large ductility of shear panel webs. However, note that flanges will be unavoidable imposed by bending moments in reality, $t_f / t_w = 4$ is recommended for practical design.

On the other hand, Fig.5 (c) shows the shear force carried by flanges is about 13–28 per cent of the total shear resistance, indicating that flanges play an important role in resisting shear force and could not be neglected in strength prediction of shear panels. The differences in the ultimate shear strength for shear panels with thicker flanges and thinner flanges are primarily due to the shear resistance carried by flanges through frame action (Vierendeel truss action). Another interesting phenomenon is that the strength of the flanges remains stable after around 5 cycles.

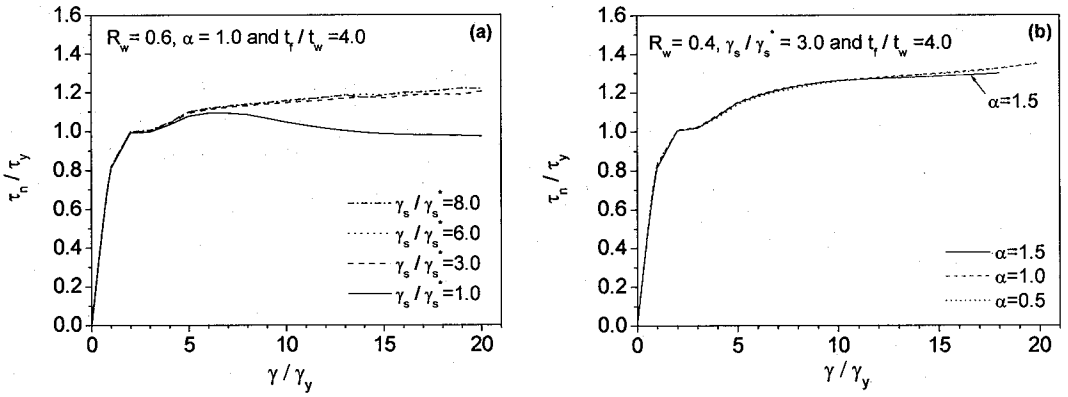

Fig.6 Effects of (a) stiffener rigidity, γ_s / γ_s^* and (b) aspect ratio, α

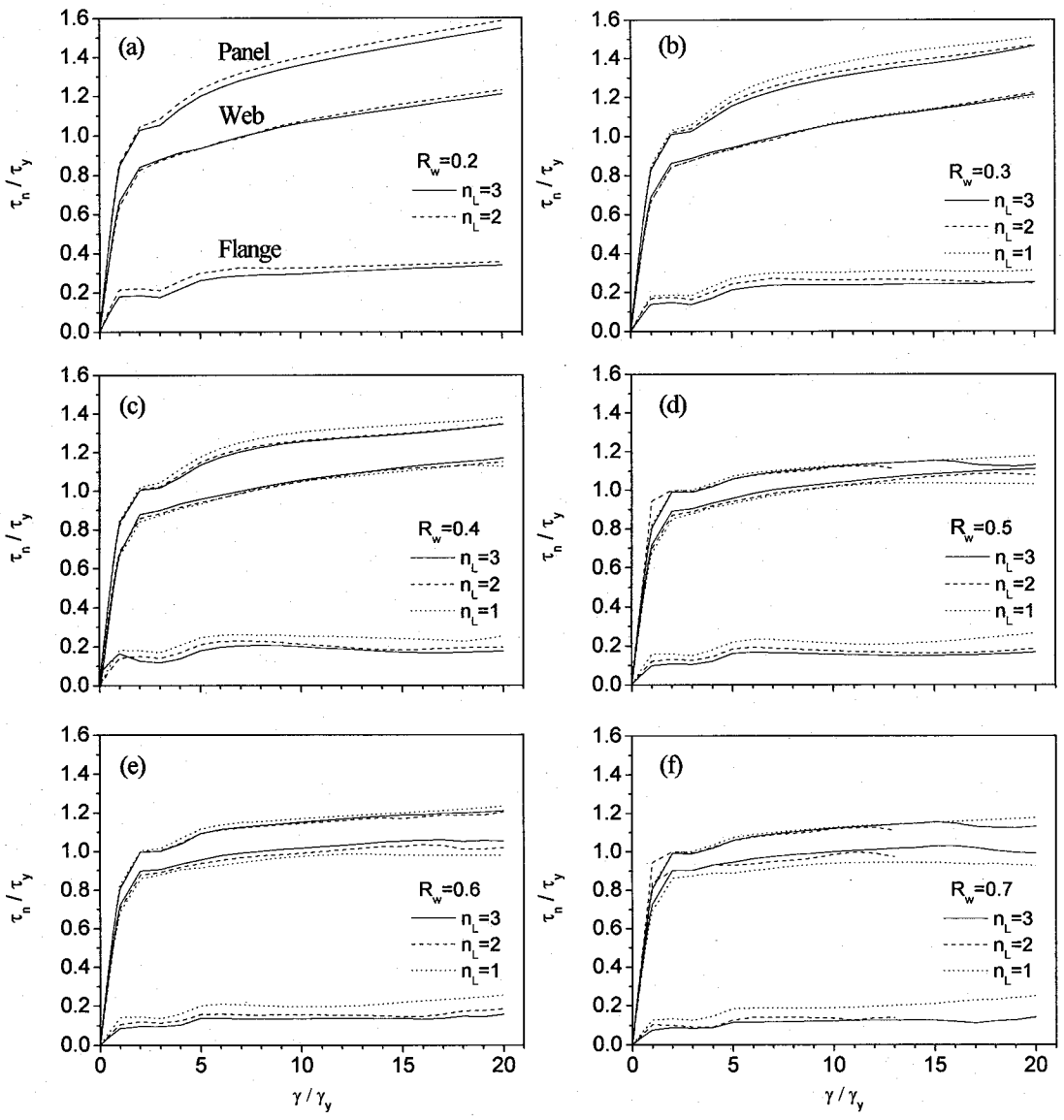

Fig.7 Effects of arrangement of longitudinal and transverse stiffeners ($\gamma_s / \gamma_s^* = 3.0$, $\alpha = 1.0$, and $t_f / t_w = 4.0$)

4.2 Effects of stiffener rigidity, γ_s / γ_s^*

Effects of stiffener rigidity are evaluated by varying the ratio γ_s / γ_s^* from 1.0 to 8.0. In earlier research studies on slender webs used in plate girders, $\gamma_s / \gamma_s^* = 1.0$ is stiff and strong enough to form the simply supported boundary of subpanels[18]. That is, stiffeners are assumed to remain straight and form the nodal line at web elastic buckling. This is demonstrated by the great agreement on the $\tau_n - \gamma$ curves for all the cases during the small deformation, as shown in Fig.6 (a). However, entering the large deformation, the case of $\gamma_s / \gamma_s^* = 1.0$ occurs strength deterioration. Comparatively, in the cases of $\gamma_s / \gamma_s^* \geq 3.0$, hysteretic behaviors are stable and agree very well with each other. Note that one of the important characteristics for shear panel dampers is to sustain severe shear deformation, $\gamma_s / \gamma_s^* = 3.0$ is considered adequate to reach the full hysteretic performance of SPD under shear. Furthermore, given $\gamma_s / \gamma_s^* \geq 3.0$, the stiffener rigidity has no influence on the ultimate shear strength of SDP.

4.3 Effects of aspect ratio, α

Range of the aspect ratio examined here is 0.5, 1.0 and 1.5, covering practical range of aspect ratio. The other parameters, R_w, γ_s / γ_s^*, t_f / t_w and a, are fixed at 0.4, 3.0, 4.0, and 1000mm, respectively.

The sensitivity of the hysteretic loop to the parameter variation is shown in Fig.6 (b). From this figure, it can be seen that the skeleton of the hysteretic loop is not susceptive to the aspect ratio except that at larger shear strain, where the envelope curve with α =1.5 has a little drop. Therefore, the effect of aspect ratio can be neglected for practical design purposes.

4.4 Effects of arrangement of longitudinal and transverse stiffeners

To further verify the above findings, the envelopes of the numerical cases, which have been summarized in Table 1, are reorganized in Fig.7. These figures are grouped according to R_w, with different arrangement of longitudinal and transverse stiffeners. In each sub-graph, the $\tau_n - \gamma$ curve denoted by "Panel" is decomposed into two components in the same manner as shown in Fig.5. One is denoted by "Web", representing the shear component being carried by the web; the other is denoted by "Flange", representing the shear component being carried by the flanges. As can be seen from Fig.7, despite of the number of stiffeners, the ultimate shear strengths of panels with equal R_w are almost the same. In each sub-graph, the maximum difference of ultimate shear strength is no more than 5 per cent. It seems that the difference is primarily due to the strength of flanges because the curves marked "Web" agree very well with each other, especially in the case of stockier and medium stockier webs. These results validate again the assumption that the web slenderness parameter, R_w, can be used as the key parameter to evaluate the hysteretic performance and ductility capacity of a stiffened shear panel. Another finding in these figures is the function of the flanges. As mentioned previously, the shear load carried by flanges remains stable after 5 cycles around. This phenomenon is observed over entire range of R_w. For stockier webs, added flange contribution to the total shear capacity can be found, whereas for slender webs, flanges make up the loss of webs' load carrying capacity. The plastic hinges are developed completely at both ends of flanges. Furthermore, plasticization is developed into the middle region of flanges. At last, the shear force carried by flanges achieves about 13–20 per cent of the total shear force. Accordingly, the importance of flange's contribution to the total shear load capacity is confirmed again.

5. Prediction of Ultimate Shear Strengths

In view of the above investigations, it is assumed that the ultimate shear strength of shear panel damper, τ_u, be composed of two parts:

$$\tau_u = \tau_{u,w} + \tau_{u,f} \tag{7}$$

where $\tau_{u,w}$ and $\tau_{u,f}$ are ultimate shear strength of web and flanges, respectively. The establishment of shear strength of web and flanges will be described as follows.

5.1 Empirical formula for shear strength of web

As demonstrated in preceding parametric study, when stiffener rigidity, flange rigidity and web aspect ratio are satisfied with suggested values, i.e. $\gamma_s / \gamma_s^* \geq 3.0$, $t_f / t_w \geq 4.0$, and $0.5 \leq \alpha \leq 1.5$, the influences of these design parameters on the web shear strength can be ignored. As a result, the ultimate shear strength of the web can be expressed by the single design parameter, R_w, given by

$$\frac{\tau_{u,w}}{\tau_y} = 0.918 + \frac{0.038}{R_w^2} \leq 1.2 \tag{8}$$

This empirical formula is proposed through least-squares method, based on the numerical analysis results. This formula is capable of predicting the web's shear strength over the range of $0.2 \leq R_w \leq 0.7$, $\gamma_s / \gamma_s^* \geq 3.0$, $t_f / t_w \geq 4.0$, and $0.5 \leq \alpha \leq 1.5$. It is noted that although Eq. (8) is applicable even for $R_w \geq 0.5$, the suitable range of $0.2 \leq R_w \leq 0.5$ is recommended for shear panel dampers, as discussed in the previous section. The strength capacity obtained from Eq. (8) as well as from Railway Technical Research Institute (RTRI)[7]

$$\frac{\tau_{u,w}}{\tau_y} = 0.6 + \frac{1.02}{3.82 R_w - 0.26} \tag{9}$$

and from Nagoya Expressway Public Corporation (NEPC)[23]

$$\frac{\tau_{u,w}}{\tau_y} = \left(\frac{0.662}{R_w} \right)^{0.333} \tag{10}$$

are plotted in Fig.8, together with numerical results from the present study and experimental results[5]. Overstrength can be

obviously observed for stockier webs. It is mainly due to the strain hardening of steel material, whose yield strength ratio is about 0.55. It is noted that Eq. (9) proposed by RTRI[7] is based on the research of Ref. 5), in which $\tau_{u,w} = \tau_u - \tau'_f$, where τ_u is experimental result of shear panels, while τ'_f is experimental result of a frame constituted of flanges and end plates only. In fact, τ'_f is smaller than the shear force actually resisted by flanges in shear panels due to neglecting the interaction of plate members. Hence, it is unavoidably overestimate $\tau_{u,w}$, especially for the smaller value of R_w. Eq. (10) proposed by NEPC[23] is applicable for web panels with two stiffeners in the middle of box sectional beam of a rigid frame. As shown in Fig.8, the curve of NEPC[23] matches well with the curve of proposed equation and the numerical results. However, Eq. (10) has no upper and lower bound.

One additional case with $n_L = n_T = 4$ is used to verify the accuracy of proposed equation, as illustrated in Fig.8. It is indicated that the equation can still be used for SPD with more than three stiffeners.

5.2 Empirical formula for shear strength of flanges

For simplicity, the shear strengths of flanges are defined as plastic hinges occur at both ends of the flanges in Guidelines presented by RTRI[7]. However, it underestimates the shear resistance of the flanges. Through pilot calculations, it is found that the numerical ultimate shear force of two flanges, V_f, has a good satisfactory linear fit to a combined factor denoted as $\sigma_{y,f} b_f t_f \left(\frac{t_f}{t_w} \cdot \frac{1}{(n_L+1)R_w\alpha} + 2 \right)$ in the form of Eq. (11), as shown in Fig.9,

$$V_f = 0.0166 \sigma_{y,f} b_f t_f \left(\frac{t_f}{t_w} \cdot \frac{1}{(n_L+1)R_w\alpha} + 2 \right) \qquad (11)$$

To be consistent with Eq. (8) in form, the predicted shear force is divided by yield shear force of the web. Since web and flanges are made of same steel material, Eq. (11) can be rearranged as,

$$\frac{\tau_{u,f}}{\tau_y} = \frac{V_f}{\tau_y b_w t_w} = 0.0287 \frac{b_f}{b_w} \cdot \frac{t_f}{t_w} \left(\frac{t_f}{t_w} \cdot \frac{1}{(n_L+1)R_w\alpha} + 2 \right) \qquad (12)$$

5.3 Comparison of design formula with numerical results

The ultimate shear strength formula developed in the preceding section is compared with the numerical results, as shown in Fig.10. It is clear that τ_u calculated from Eq. (7) in conjunction with Eqs. (8) and (12) yields good agreement within an error of 10 per cent. On the other hands, overstrength can be observed in Fig. 10. Such overstrength is mainly contributed to the shear resistance of the flanges, which needs to be carefully considered either in design of supporting braces linked with dampers or in establishing a more appropriate overstrength factor in damper design.

6. Development of Hysteretic Model for Stiffened Steel SPD

According to the above analytical results, a simplified bilinear restoring model is proposed to simulate the hysteretic behavior of stiffened shear panels used as passive energy dissipating dampers. Fig.11 (a) shows the schematic of the bilinear model with kinematic hardening rule for shear dampers made of steel grade SS400. The first point is (τ_y, γ_y), and the second point is the ultimate shear strength, τ_u, at $\gamma_u = 20\gamma_y$, where τ_u is given by Eq. (7). As shown previously, the shear panel damper is of good ductility up to $20\gamma_y$ when $R_w \leq 0.5$. Note that the first stiffness, K, is equal to elastic shear module, G, while the second stiffness, K_s,

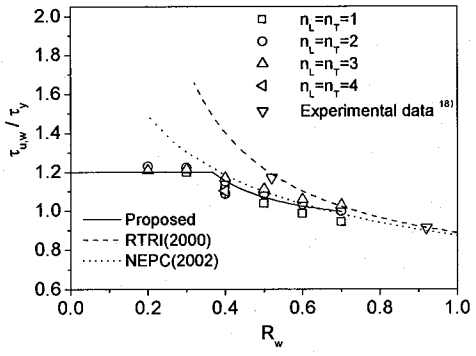

Fig.8 Strength comparison of stiffened webs under shear

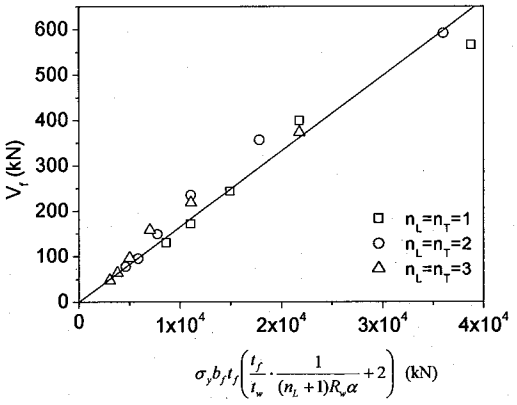

Fig.9 Shear force resisted by flanges

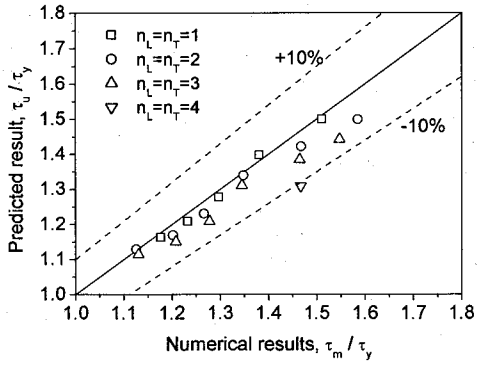

Fig.10 Comparison of ultimate shear strength between numerical and predicted results

is about 1–3 per cent of K, where $K_s = (\tau_u / \tau_y - 1)/19$. As an example, Fig.11 (b) represents the comparison of hysteretic loops from the proposed bilinear model and numerical analysis with $R_w = 0.4$. As an energy dissipator, one of the most important indexes to evaluate the performance of energy dissipating devices is cumulative energy dissipation. Here, dissipated energy, E_i, is normalized by E_e, defined as $Q_y \Delta_y/2$. The normalized dissipated energy, E_i / E_e, is twice of the area A_i, which is calculated for each cycle from positive to negative as shown in Fig.12. The cumulative dissipated energy is defined as the sum of previous dissipated energy, $\Sigma E_i / E_e$. The total cumulative dissipation energy of all cases is summarized in Table 1 and the comparison of corresponding cumulative dissipated energy at each cycle between proposed bilinear model and numerical results is shown in Fig.13. It can be seen that the proposed bilinear model can dissipate almost the same energy as numerical results with errors less than 15 per cent.

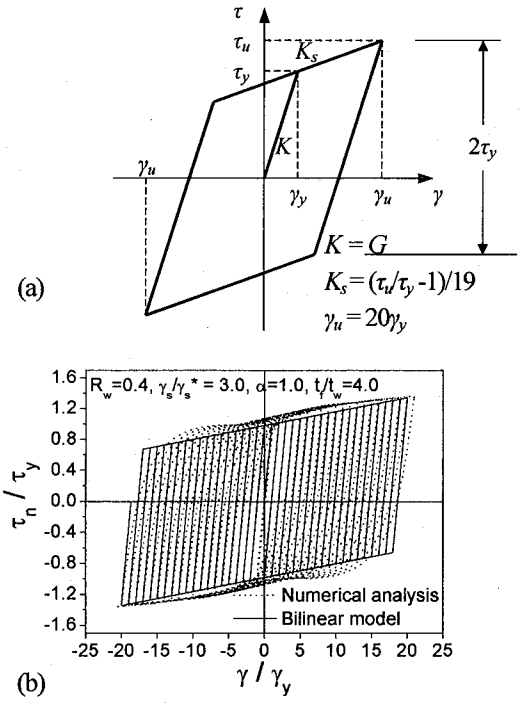

Fig.11 Shear panel damper: (a) bilinear model; (b) hysteretic curves from proposed bilinear model and numerical analysis

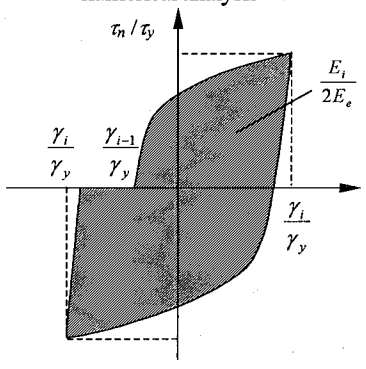

Fig.12 Definition of dissipated energy in each cycle, E_i / E_e

7. Conclusions

An extensive analytical study has been conducted on two-way stiffened shear panels. Investigations of general shear hystereticbehavior and comprehensive sensitivity studies have been carried out. Some main findings are concluded as follows:

1. For the shear panels used as passive energy dissipating devices, $0.2 \le R_w \le 0.5$, $\gamma_s / \gamma_s^* \ge 3.0$, $t_f / t_w \ge 4.0$, and $0.5 \le \alpha \le 1.5$ are recommended for shear panel dampers in practical design. Within these ranges, the web yields in full plastic manner before it buckles, pinch is avoided and excellent ductility up to the low-fatigue limit of $\gamma_u = 20\gamma_y$ can be guaranteed.
2. To predict the ultimate shear strength capacity, not only web but also flanges must be considered to resist reversal of shear loads. Especially in the case of stockier webs, a shear force component resisted by flanges is about 20 per cent of the total shear strength.
3. An empirical formula is proposed to predict the ultimate shear strength of shear panel dampers, as a summation of ultimate shear strength of web and flanges obtained from Eq. (8) and Eq. (12).

A simple yet accurate bilinear restoring model is proposed to represent the hysteretic behavior of stiffened shear panel dampers. The proposed model is expected to get use in time-history analysis of structural system installed with such type of shear panel damper.

References

1) Housner, G. W., Bergman, L. A., Caughey, T. K., Chassiakos, A. G., Claus, R. O., Masri, S. F., Skelton, R. E., Soong, T. T., Spencer, B. F., and Yao, J. T. P., Structural control: past, present, and future, *J. Eng. Mech.*, ASCE, 123(9), pp.897-971, 1997.

2) Nakashima, M., Iwai, S., Iwata, M., Takeuchi, T., Konomi, S., Akazawa, T., and Saburi, K., Energy dissipation behavior of shear panels made of low yield steel, *Earthquake Eng. Struct. Dyn.*, 23(12), pp.1299-1313, 1994.

3) Tanaka, K. and Sasaki, Y., Hysteretic performance of shear panel dampers of ultra low-yield-strength steel for seismic response control of buildings, 12WCEE (CD-Rom), Aucklan, NZ, 2000.

4) Nakashima, M., Strain-hardening behavior of shear panels made of low-yield steel. I: Test, *J. Struct. Eng.*, ASCE, 121(12), pp.1742-1749, 1995.

5) Takahashi, Y. and Shinabe, Y., Experimental study on restoring force characteristics of shear yielding thin steel plate elements, *J. Struct. Constr. Eng.*, AIJ, 494, pp.107-114, 1997.

6) Tanaka, K., Sasaki, Y., and Yoneyama, S., An experimental study on hysteretic performance of shear panel dampers using different strength type of steel under static loading, *J. Struct.*

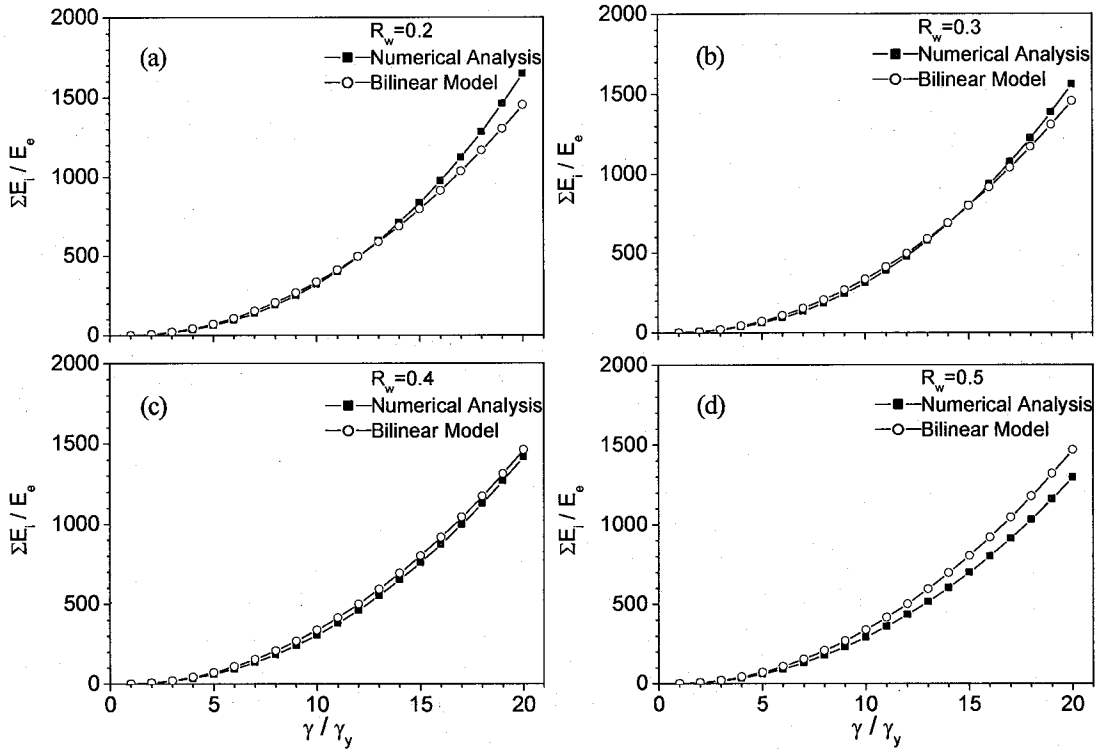

Fig.13 Comparison of cumulative dissipated energy between proposed bilinear model and numerical results (n_L=n_T=2, γ_s/γ_s*=3.0, α=1.0 and t/t_w=4.0)

Constr. Eng., AIJ, 520, pp.117-124, 1999.

7) Railway Technical Research Institute (RTRI), *Guidelines for Design of Railway Viaduct with Dampers and Braces*, RTRI, Tokyo, 2000.

8) McDaniel, C. C., Uang, C. M., and Seible, F., Cyclic testing of built-up steel shear links for the new bay bridge, *J. Struct. Eng.*, ASCE, 129(6), pp.801-809, 2003.

9) JIS G3101, *Rolled steels for general structure, Japanese Standards Association*, Tokyo, 2004.

10)ASTM A6/A6M-05, *Standard Specification for General Requirements for Rolled Structural Steel Bars, Plates, Shapes, and Sheet Piling*, American Society of Testing and Materials, PA, 2005.

11)Chusilp, P. and Usami, T., New elastic stability formulas for multiple-stiffened shear panels, *J. Struct, Eng.*, ASCE, 128(6), pp.833-836, 2002.

12)Shen, C., Mamaghani, I. H. P., Mizuno, E., and Usami, T., Cyclic behavior of structural steels. II: theory, *J. Eng. Mech.*, ASCE, 121(11), pp.1165-1172, 1995.

13)Shen, C., Mizuno, E., and Usami, T., *Development of a Cyclic Two-Surface Model for Structural Steels with Yield Plateau*, NUCE Res. Rep. No. 9302, Department of Civil Engineering, Nagoya University, Nagoya, 1993.

14)Fukumoto, Y., ed., *Guidelines for Stability Design of Steel Structures*, Subcommittee on Stability Design, Committee on Steel Structures, Japan Society of Civil Engineers, Tokyo, 1987.

15)BSI, BS5400, Part3, 1980.

16)*ABAQUS*, Inc., ABAQUS/Analysis user's manual–version 6.4. Pawtucket, R.I., 2003.

17)Gao S. B., Usami, T., and Ge, H. B., Ductility evaluation of steel bridge piers with pipe sections, *J. Eng. Mech.*, ASCE, 124(3), pp.260-267, 1998.

18)Chusilp, P., Usami, T., Ge, H. B., Maeno, H., and Aoki, T., Cyclic shear behavior of steel box girders: experiment and analysis, *Earthquake. Eng. Struct. Dyn.*, 31(11), pp.1993-2014, 2002.

19)Chusilp, P., *Seismic Design Methodology for Steel Bridge Structures with Shear-type Hysteretic Dampers.* Thesis, presented to Nagoya University, Japan, in partial fulfillment of the requirements for the degree of Dr. of Engineering, 2002.

20)Usami, T. and Ge, H. B., Strength prediction of thin-walled plate assemblies, *J. Struct. Eng.*, JSCE, 42A, pp.171-178, 1996.

21)Kasai, A., Watanabe, T., Amano, M., and Usami, T., Strength and ductility evaluation of stiffened steel plates subjected to cyclic shear loading, *J. Struct. Eng.*, JSCE, 47A, pp.761-770, 2001.

22)Porter, D. M., Rockey, K. C., and Evans, H. R., The collapse behavior of plate girders loaded in shear, *The Struct. Eng.*, London, 53(8), pp.313-325, 1975.

23)Nagoya Expressway Public Corporation (NEPC), *Seismic Performance Evaluation Criteria for Partially Concrete-Filled Steel Piles (Proposal)*, Nagoya, Japan, 2002.

(Received September 10, 2005)